RSC Advances

PAPER

View Article Online
View Journal | View Issue

Cite this: *RSC Adv.*, 2024, **14**, 37774

Nanoscale-surface roughness enhances the performance of organic thin-film thermoelectrics†

Balwinder Kaur,[ac] Ezaz Hasan Khan,[ac] Anna Maria Routsi,[ad] Lian Li,[bc] Andrew Latulippe,[e] Hongwei Sun,[e] Christopher Drew,[f] Jayant Kumar*[bc] and Dionysios C. Christodouleas *[a]

Organic thermoelectric materials would be ideally suited for wearable thermoelectric devices but currently are not efficient enough for practical applications. Previous research efforts have tailored the composition, oxidation status, or doping levels of organic thin-film thermoelectrics to maximize their thermoelectric performance typically measured by the thermoelectric figure of merit (*ZT*). This study demonstrates that the thermoelectric *ZT* of the organic thin-films can be significantly boosted by increasing the surface roughness of the films. A simple soft-templating method that can produce nanorough thin films of organic thermoelectrics was developed and used to fabricate nanorough poly(3,4-ethylenedioxythiophene):Tosylate (PEDOT:Tos) thin films. The performance of the nanorough PEDOT:Tos films was compared to that of the smooth PEDOT:Tos films. The *ZT* value of the nanorough films was estimated to be 0.99, which is 83% higher than that of the smooth films and one of the highest ever reported for organic thermoelectrics. The flexibility and durability of the nanorough PEDOT:Tos films were also proved. A proof-of-concept thermoelectric device that used 5 strips of nanorough films, as the p-type thermoelectric elements, and five strips of bismuth thin films, as the n-type elements, produced 118.7 nW when $\Delta T = 50$ K.

Received 24th June 2024
Accepted 6th November 2024

DOI: 10.1039/d4ra04591b

rsc.li/rsc-advances

Introduction

Thermoelectric generators (TEG) are devices that use the temperature difference between two bodies/objects to generate electric energy (due to the Seebeck effect) and to power an electronic device. Humans are homeotherms and their skin temperature is stable (typically around 32 °C when properly protected). The temperature of the surrounding air (especially on cold days) could be several degrees different than that of human's skin, therefore, wearable thermoelectric generators, if efficient enough, could use this temperature difference to power electronic devices with low power demand (*e.g.*, health sensors, wearables, smart devices *etc.*).

To find practical applications, wearable thermoelectric generators need to be efficient but also inexpensive, lightweight, non-toxic, and flexible. The majority of previous studies have used inorganic alloys, *e.g.*, bismuth telluride, for the fabrication of proof-of-concept wearable thermoelectric devices.[1–3] Bismuth telluride and other similar inorganic alloys, however, are rigid and considered to be toxic and skin irritants[4] so they need to be encapsulated inside polydimethylsiloxane (PDMS) structures to be used for conformable and wearable devices.[2,5] Organic thermoelectric materials (*i.e.*, thin films of conducting polymers,[6–8] composites of conducting polymers with carbonaceous materials (*e.g.*, carbon nanotubes, graphene), inorganic nanomaterials, or ionic liquid[6–12] composites of conducting polymers with paper[13] or fabrics[14]) are non-toxic, lightweight, and compatible with clothing so they would be ideal for wearable thermoelectrics if they could be efficient enough.

The thermoelectric efficiency of materials is usually evaluated by calculating the dimensionless thermoelectric figure of merit, *ZT*; $ZT = S^2\sigma T/k$, where σ, S, k and T are electrical conductivity, Seebeck coefficient, thermal conductivity, and average absolute temperature during testing, respectively. To maximize the thermoelectric efficiency of thin-film organic thermoelectrics, previous research efforts have tailored films' oxidation state[5,15,16] (that theoretically influences σ, S and k), and composition[15,17–20] (that affect σ and k). For example, several studies on poly(3,4-ethylenedioxythiophene):Tosylate (PEDOT:Tos) films have shown that the thermoelectric properties of the PEDOT:Tos films can be altered by post-treating the films with

[a]*Department of Chemistry, University of Massachusetts Lowell, Lowell, MA 01854, USA. E-mail: Dionysios_Christodouleas@uml.edu*

[b]*Department of Physics and Applied Physics, University of Massachusetts Lowell, Lowell, MA 01854, USA. E-mail: Jayant_Kumar@uml.edu*

[c]*Center for Advanced Materials, University of Massachusetts Lowell, Lowell, MA 01854, USA*

[d]*Core Research Facilities, University of Massachusetts Lowell, Lowell, MA 01854, USA*

[e]*Department of Mechanical Engineering, University of Massachusetts Lowell, Lowell, MA 01854, USA*

[f]*U.S. Army Combat Capabilities Development Command Soldier Center (DEVCOM SC), Natick, MA 01760, USA*

† Electronic supplementary information (ESI) available. See DOI: https://doi.org/10.1039/d4ra04591b

acid/base solutions[18] or a reducing agent.[21] Kim *et al.* have prepared PEDOT:Tos films that also contained triblock copolymers and tailored the oxidation state of the films using an electrochemical treatment step.[15] Petsagkourakis *et al.* prepared PEDOT:Tos films that also contained high boiling point solvents as additives (*e.g.*, DMSO, DMF) to increase films' crystallinity and electrical conductivity.[20] The surface morphology of the thin films should, in principle, also influence the thermoelectric efficiency (by affecting mainly k) of thin-film organic thermoelectrics, but there are no published studies that have examined this hypothesis.

To test the hypothesis that increased surface roughness leads to enhanced thermoelectric performance in thin-film organic thermoelectrics, we prepared smooth and nanorough thin films of PEDOT:Tos on poly(ethylene terephthalate) (PET) sheets. We selected PEDOT:Tos as the model case of thin-film organic thermoelectrics because PEDOT:Tos thin films exhibit the highest thermoelectric efficiency among other thin films of organic conductive polymers (*e.g.*, polyaniline, polypyrrole, poly(2,5-dimethoxyphenylenevinylene), poly(2,5-diethoxyphenylenevinylene)-poly(phenylenevinylene) *etc.*).[22–25] We used PET sheets as the solid substrate of the thin films because PET sheets are lightweight, flexible, inexpensive, compatible with clothing/textiles, and exhibit low thermal conductivity (equal to 0.15 W m^{-1} K^{-1}).[26] We fabricated the nanorough PEDOT:Tos films using a new soft templating method that we describe herein. For comparison reasons, we also prepared PEDOT:Tos films with similar composition to that of nanorough films but with a smooth surface. We measured the electrical conductivity, Seebeck coefficient, and cross-plane thermal conductivity of both the smooth and nanorough films and we calculated the power factor, P, and an estimate of the figure of merit, ZT, of the films. We also measured the actual power produced from strips of the nanorough thermoelectric films at several temperature gradients and tested their durability by performing bending, creasing, adhesion, and washing tests. To further explore how much power a PEDOT-based thermoelectric device can produce under realistic conditions, we developed a proof-of-concept complete thermoelectric device that was composed of strips of nanorough PEDOT:Tos and strips of bismuth films. We measured the potential difference and actual power produced by the device when various temperature differences were applied on the opposite sides of the device.

Experimental design

New soft-templating method for fabricating nanorough thin films of PEDOT:Tos

PEDOT-based thin-film thermoelectrics are typically fabricated by spin-coating the PEDOT or the monomer mixture onto a substrate[7,27] or by using vapor phase polymerization.[5] In both cases, the surface of the thin films is relatively smooth. The soft-templating method we developed at first prepares a thin film of PEDOT:Tos (on a PET sheet) that has polystyrene nanobeads embedded. Then the polystyrene nanobeads are dissolved and leave behind nanovoids that make the surface of the PEDOT:Tos films rough. Even though we tested the performance of the soft template method towards the fabrication of only nanorough PEDOT:Tos films, we believe that this technique can be also used for the preparation of nanorough films of other organic conducting polymers prepared using *in situ* polymerization of a monomer solution or vapor phase polymerization.

In brief, the main steps of the soft-templating method were the following (Fig. 1): (A) a PET sheet was first plasma treated to introduce hydroxyl and carboxyl groups on the surface of the sheet. (B) The plasma treated PET sheet was treated with poly(diallyldimethylammonium chloride) (PDAC) to allow the immobilization of PDAC layers on top of PET and the formation of PDAC/PET composite. (C) Carboxylated polystyrene nanobeads were drop-casted on the PDAC/PET composite film and were stuck on the surface of the film due to electrostatic interactions between the negatively charged nanospheres and the positively charged PDAC present on the film; nanospheres had a mean diameter around 200 nm because preliminary experiments have shown that larger nanospheres flied off the substrate during a subsequent spin coating step, while smaller spheres could not be dissolved at a later step because they were totally embedded within the films. (D) A mixture of EDOT, catalyst (*i.e.*, iron(III) tris-*p*-toluenesulfonate), and pyridine was spin-coated on the nanobeads/PDAC/PET substrate and the films were placed in an oven to allow the *in situ* polymerization of the mixture and the formation of a thin film of PEDOT:Tos (that has nanobeads embedded). (E) The film was washed with chloroform to dissolve the embedded nanospheres[28] and result in a nanorough PEDOT:Tos thin film on the PDAC/PET substrate. The detailed experimental protocol is depicted in Fig. S1 and described in the ESI.†

Preparation of smooth thin films of PEDOT:Tos

For comparison reasons, we also fabricated smooth PEDOT:Tos thin films using an experimental protocol that had several

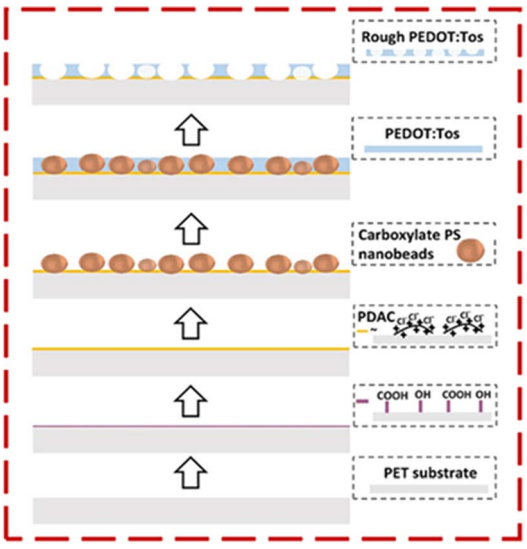

Fig. 1 Schematic representation of the preparation of nanorough PEDOT:Tos/PDAC films on a PET sheet.

identical steps to the protocol used for the fabrication of the nanorough films. More specifically, smooth PEDOT:Tos/PDAC/PET films were prepared following exactly the same steps described above except for the one that included the immobilization of the nanobeads onto the PDAC/PET substrate (see the ESI† for the detailed protocol).

Determination of morphology and thermoelectric properties of the PEDOT:Tos films

The morphology and thickness of the PEDOT:Tos thin films were measured by atomic force microscopy (AFM) and field-emission scanning electron microscopy (FE-SEM). The Seebeck coefficient was determined by employing a thermoelectric heater and a thermoelectric cooler in conjunction with two T-type thermocouples and an electrometer. To minimize the error of the measured values, the voltage difference was measured at the same point of the thermal contact. The Seebeck coefficient was calculated from the slope of the plot of temperature gradient *vs.* voltage. The electrical conductivity was measured by using the standard four-point probe method.

The cross-plane thermal conductivity, $\boldsymbol{k}_{\perp}$, of the smooth and nanorough PEDOT:Tos/PDAC/PET films was measured by fabricating multi-layered composite structures that contain the tested film (Fig. S2†) and by using the 3ω method (see ESI for details†). To verify the ability of the used approach to get accurate estimates of the cross-plane thermal conductivity of tested materials, we also measured the cross-plane thermal conductivity of PDMS samples. The measured cross-plane thermal conductivity of PDMS samples ($\boldsymbol{k}_{\perp} = 0.18$ W m^{-1} K^{-1}) was close to the value ($\boldsymbol{k}_{\perp} = 0.15$ W m^{-1} K^{-1}) reported in the literature,[29] reassuring us about the validity of the results of the testing methodology.

Typically the in-plane thermal conductivity, $\boldsymbol{k}_{\parallel}$, of sub-micrometer thick organic thermoelectric films is calculated indirectly from the measured value of $\boldsymbol{k}_{\perp}$ the thin film and the ratio of $\boldsymbol{k}_{\parallel}/\boldsymbol{k}_{\perp}$ calculated by testing micrometer-thick films that have the same composition and prepared using the same experimental protocol.[16] Micrometer-thick nanorough PEDOT:Tos/PDAC/PET films, however, cannot be prepared using our soft templating method because of the limited dissolution of the polystyrene spheres when the films are thicker than 200 nm. Given that the PEDOT:Tos films prepared in this study have similar composition to the films prepared by Bubnova *et al.*[16] and they were also produced by *in situ* polymerization of a spin coated thin film of a monomer mixture, we speculated that they would also exhibit a similar ratio of $\boldsymbol{k}_{\parallel}/\boldsymbol{k}_{\perp} = 1.1$.[16] We therefore calculated an estimate of the in-plane thermal conductivity of the films from $\boldsymbol{k}_{\parallel} = 1.1 \times \boldsymbol{k}_{\perp}$. The ESI† section includes more information about the thermal conductivity measurements and the obtained results.

Determination of durability of PEDOT:Tos films

The durability of the nanorough PEDOT:Tos/PDAC/PET composite films was examined by measuring the thermoelectric properties of the nanorough PEDOT:Tos films before and after performing several cycles of creasing, bending, adhesion, and washing tests. The creasing test was performed by creasing the nanorough PEDOT:Tos/PDAC/PET composite film and checking the electrical resistance before and after the test. The bending test was carried out by rolling pieces of nanorough PEDOT:Tos films (1.5 cm × 1.5 cm) around a cylindrical rod with radius between 1 and 5 mm. The adhesion of nanorough PEDOT:Tos films on PET was tested by adhering and peeling scotch tapes repeatedly. The washing cycles of the nanorough PEDOT:Tos films consisted of soaking in soap water and then clean water followed by drying in hot air.

Design and fabrication of a complete thermoelectric device

To explore how much power a PEDOT-based thermoelectric device can produce in realistic conditions, we developed a proof-of-concept complete thermoelectric device (Fig. 2A and B) that was composed of five strips of p-type organic thermoelectric material (*i.e.*, nanorough PEDOT:Tos/PDAC/PET) and five strips of n-type thermoelectric material (*i.e.*, bismuth films deposited on PET films, Bi/PET). We used a programmable auto cutter to fabricate the device, so the protocol was semi-automatic and could be potentially easily scaled up. More specifically, the width of each strip and distance between the two electrodes of each strip was kept at 1 cm and 2 cm, respectively. The auto cutter was programmed to cut a nanorough PEDOT:Tos/PDAC/PET sheet straight and parallel (Fig. S3†) whereas Bi/PET sheet was cut

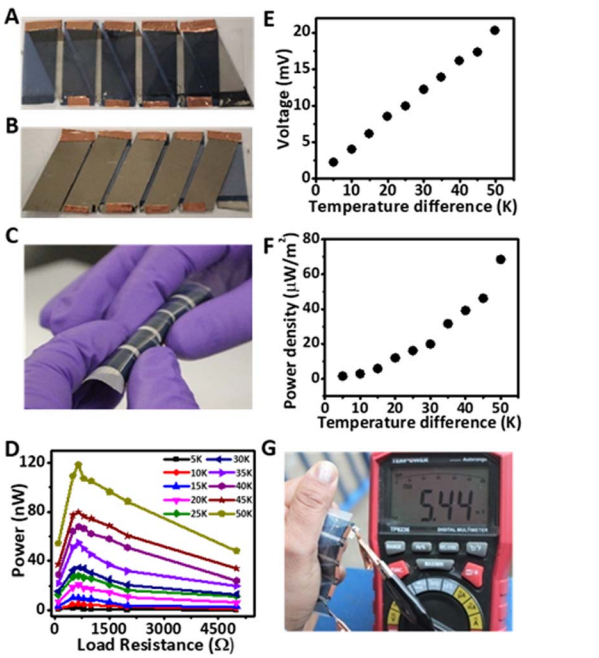

Fig. 2 (A and B) Photos of the complete thermoelectric device from both sides; the nanorough PEDOT:Tos/PDAC/PET strips (p-type elements) are at top in (A) and the bismuth/PET strips (n-type elements) are at top in (B). (C) Photo of the complete TE device being bended. (D) Total output power produced by the device as a function of load resistance and temperature difference between cold and hot sides. (E) Voltage developed across the device as a function of temperature difference. (F) Maximum power density obtained as a function of temperature difference. (G) Photo of the complete thermoelectric device operating at an ambient temperature of 15 °C.

slightly tilted so that one edge of Bi/PET would join one nano rough PEDOT:Tos/PDAC/PET strip and second edge of Bi/PET would join adjacent nanorough PEDOT:Tos/PDAC/PET strip (Fig. S3†). After cutting the nanorough PEDOT:Tos/PDAC/PET and Bi/PET sheets with an auto cutter, the two sheets were attached together using silver paste by placing the Bi/PET on the top of the nanorough PEDOT:Tos/PDAC/PET as shown in Fig. S3.† A nylon fabric was placed between two sheets to avoid the direct contact between the nanorough PEDOT:Tos/PDAC and Bi films. Finally, the joined nanorough PEDOT:Tos/PDAC/PET and Bi/PET sheets were cut from both edges leaving behind the Bi/PET strips joined with alternate nanorough PEDOT:Tos/PDAC/PET strips through silver paste only. The complete thermoelectric device was flexible, conformable (Fig. 2C) and had a footprint of 17.29 cm^2.

To get an estimate of the power output that the nano rough PEDOT:Tos/PDAC/PET films may produce, we measured the actual power (in nW) produced from strips (of various dimensions) of the nanorough thermoelectric films at several temperature gradients and with different external loads. More specifically, we used heating and cooling elements (hot plates, Peltier elements *etc.*) to force the opposite sides of the device to be at different temperatures and then connected the device to an external circuit that contains an external load resistor (Fig. S4†). We then measured the electrical current (I) that flows through the external load resistor (R) and measured the power output from $P_{out} = I^2R$.

Results and discussion

Morphology and thermoelectric properties of PEDOT:Tos films

AFM and SEM images indicated that the surface morphology of the nanorough PEDOT:Tos/PDAC/PET films is distinctively different to that of the smooth films (Fig. 3A–D). More specifically, the surface of the nanorough films exhibits crater-like nanovoids with diameters ranging between 100 and 1000 nm (Fig. S5†); the crater-like nanovoids are distributed almost uniformly on the surface of the films. The total thickness of the thin films was measured from the AFM height profiles (Fig. 3E and F) and was found to be equal to 210 ± 5 nm for the nanorough films and 232 ± 7 nm for the smooth films. The root mean square (RMS) roughness of the nanorough films was estimated to be equal to 34 ± 5 nm that is 80% higher than that of the smooth films (that was 19 ± 2 nm). The roughness average, R_a, was equal to 31 ± 3 nm for the nanorough films and 15 ± 2 nm for the smooth films.

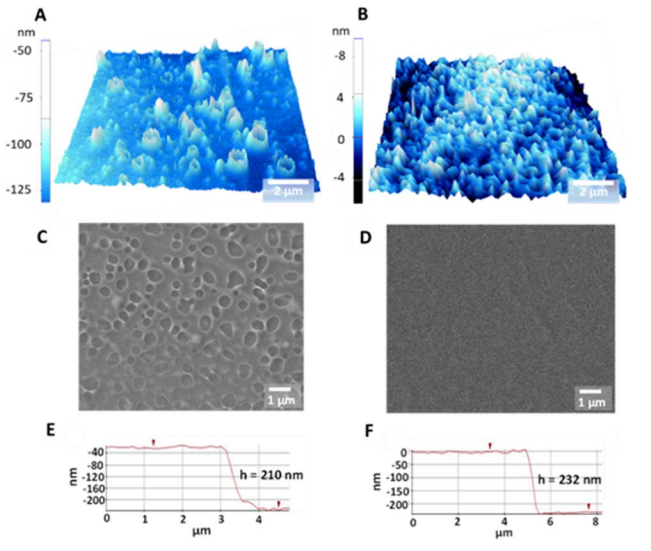

Fig. 3 3D AFM images of a nanorough (A) and a smooth (B) PEDOT:Tos/PDAC/PET film. SEM images of a nanorough (C) and a smooth (D) PEDOT:Tos/PDAC/PET films. AFM height profiles indicating the film thickness of a nanorough (E) and a smooth (F) PEDOT:Tos/PDAC/PET film.

Table 1 shows the calculated values of the electrical conductivity, Seebeck coefficient, and cross-plane thermal conductivity, $\boldsymbol{k}_\perp$, of the smooth and nanorough PEDOT:Tos/PDAC/PET films. Table 1 also includes the estimated values of the in-plane thermal conductivity, $\boldsymbol{k}_\parallel$, figure of merit, ZT, and power factor, PF = $S^2\sigma$. The nanorough PEDOT:Tos/PDAC/PET films exhibited $\boldsymbol{k}_\perp$ = 0.18 W m^{-1} K^{-1} that is 38% lower than that of smooth films ($\boldsymbol{k}_\perp$ =0.30 W m^{-1} K^{-1}) (Table S1†). It should be noted that the estimated $\boldsymbol{k}_\perp$ of smooth PEDOT:Tos/PDAC/PET ($\boldsymbol{k}_\perp$ =0.30 W m^{-1} K^{-1}) is close to the value ($\boldsymbol{k}_\perp$ =0.33 W m^{-1} K^{-1}) reported by Bubnova *et al.*[16] This is actually the first experimental evidence that nanoscale surface roughness affects the thermal conductivity of organic thermoelectric thin films. Similar correlation between thermal conductivity and surface roughness was previously reported only in the case of nanostructured inorganic thermoelectrics.[30–33] The $\boldsymbol{k}_\parallel$ of the nanorough PEDOT:Tos/PDAC/PET films was estimated equal to 0.20 W m^{-1} K^{-1}.

The low thermal conductivity of the nanorough films could be attributed either to low k_e (the electronic component of k) or low k_L (the lattice component of k); $k_{total} = k_e + k_L$. The exact contribution of k_e and k_L to k in the case of conducting polymers has not been well established and there are many open questions.[34] Even the validity of Wiedemann–Franz law that implies that the k_e is proportional to σ is questionable;[35,36] Bubnova *et al.* actually hypothesized that k is independent of σ.[16] Nanorough PEDOT:Tos/PDAC/PET films exhibited lower k than smooth films while they also exhibited higher σ (see Table 1), so if we assume the validity of the Wiedemann–Franz law then the electronic contribution k_e should be small and the lattice contribution k_L should determine k_{total}. The lattice contribution k_L is influenced by several mechanisms (*e.g.*, phonon–phonon scattering, phonon confinement, and phonon boundary scattering *etc.*)[37] but none study has examined in detail films of conductive polymers. Thus no specific speculation can be proposed as the most likely to occur on thin films of organic thermoelectrics with nanorough surface.

Besides the low k, nanorough PEDOT:Tos/PDAC/PET films also exhibit relatively high σ which could be mainly attributed to the treatment of PET substrate with the cationic polyelectrolyte PDAC prior to the *in situ* polymerization of PEDOT:Tos and the use of an optimized ratio of oxidant-monomer-base for the *in situ* polymerization.

Table 1 Comparison of the electrical conductivity, Seebeck coefficient, power factor, and figure of merit of various PEDOT:Tos films ($N = 3$)

Sample information	Electrical conductivity (S cm^{-1})	Seebeck coefficient (μV K^{-1})	Cross-plane thermal conductivity (W m^{-1} K^{-1})	In-plane thermal conductivity (W m^{-1} K^{-1})[a]	Power factor (PF) (μW m^{-1} K^{-2})	Figure of merit (ZT) ($T = 310$ K)
Nanorough PEDOT:Tos/PDAC/PET	1000 ± 21	80.1 ± 2.5	0.18 ± 0.01	0.20	642	0.99
Smooth PEDOT:Tos/PDAC/PET	892 ± 28	80.2 ± 1.6	0.30 ± 0.01	0.33	574	0.54
Smooth PEDOT:Tos/PET	708 ± 23	78.6 ± 2.3	N.D	N.D	437	0.41[b]
Smooth PEDOT:Tos/PET[c]	625 ± 18	78.5 ± 2.1	N.D.	N.D	385	0.36[b]
Smooth PEDOT:Tos/glass[b,c]	390 ± 16	60.8 ± 1.9	N.D	N.D	144	N.D

[a] The values are calculated from cross plane thermal conductivity values and by assuming that $\boldsymbol{k}_{\parallel}/\boldsymbol{k}_{\perp} = 1.1$. [b] ZT was calculated using the in plane thermal conductivity of smooth PEDOT:Tos/PDAC/PET. [c] Films were not treated with chloroform.

The influence of the solid substrate to the performance of organic thin-film thermoelectrics is not well understood. Supplementary experiments performed herein (see ESI for details)† suggest that the nature of the substrate could influence the electrical conductivity σ of the films. For example, smooth PEDOT:Tos films deposited on PET exhibited 167% higher power factor than smooth PEDOT:Tos films deposited on glass (Table 1). One possible explanation is that the polymeric nature of PET substrates might allow the formation of larger grains and uniform highly conducting thin PEDOT films while the hydrophilic glass substrates might exhibit highly resistive islands of PEDOT.[38] Supplementary experiments (see ESI for details)† have also shown that the presence of the PDAC layer on the PET substrate enhance σ by 20% (Table 1). Polyelectrolytes are known to enhance the Seebeck coefficient of PEDOT-based thermoelectric films[39] but this is the first experimental report to demonstrate that a polyelectrolyte can also increase the σ of PEDOT-based films. We speculate that this increase is attributed to the interaction of tosylate with PDAC that may lead to better in plane alignment of PEDOT chains.

The ZT of nanorough PEDOT:Tos/PDAC/PET films was calculated equal to 0.99 (at 310 K) which is one of the highest ZT ever reported for PEDOT-based films and composites (see Table S2†) and even higher than the ZT of several inorganic alloys based on bismuth telluride.[40,41] The ZT of the nanorough PEDOT:Tos/PDAC/PET films is actually more than two times higher than the ZT of the pristine PEDOT:Tos/PET films prepared herein (Table 1) or reported in the literature.[16,27–42]

The power factor of the nanorough PEDOT:Tos/PDAC/PET films was determined to be 642 μW m^{-1} K^{-2} that is the highest value ever reported for pristine PEDOT:Tos films and one of the highest for organic thermoelectrics in general (Table S2†).

It should be noted, however, that when both power factor and ZT values are available, ZT provides a better measure of the thermoelectric properties of the materials. This is because power factor may overestimate the thermoelectric properties of the tested materials, as it does not take into consideration the influence of thermal conductivity on the thermoelectric properties. For example, pure silver films exhibit power factor values up to 2666 μW m^{-1} K^{-2} ($\sigma = 6.30 \times 10^7$ S m^{-1} and $S = 6.5$ μV K^{-1}) but are not good thermoelectric materials because they cannot maintain temperature gradients necessary to produce power for extended time due to the very high thermal conductivity of silver.

The actual power (in nW) produced from strips of the nanorough thermoelectric films at several temperature gradients is shown in Fig. 2D. The measured power was influenced, as expected,[43] by the temperature gradient but also by the dimensions of the films (Table S3†) and the external load used during testing (Fig. 2D, and Table S4†). Table S3† shows that (even though all the films exhibited the same ZT) the output power varies significantly (between 2.17 and 0.25 nW) and depends on the geometric characteristics of the films; longer elements produced less power than the shorter ones because a portion of the produced power was consumed inside the thermoelectric element due to its internal resistance. Importantly, strips of the nano rough PEDOT:Tos/PDAC/PET films that are up to 2 cm long can still produce around 2 nW of power (at a ΔT of 10 K) that could allow the fabrication of thermoelectric devices where the cold and hot sides are few centimeters apart. For comparison, Bulova *et al.* has prepared a thermocouple that has a 3 μm thick pillar of PEDOT/Tos and a 3 μm thick pillar of carbon black and measured a maximum power output of 1.13 nW when ΔT was set at 1.5 K.[16] Typically, the majority of thermoelectric elements reported in the literature are less than 2 mm long or 2 mm thick[15,16,44,45] even if temperature differences of tens of degrees in very close proximity are very uncommon under ambient conditions and they could not be sustained for a long time.[46] Table S4† shows the dependence of the output power on the external load. As expected output power reaches a maximum when the load resistance approximates the internal resistance of the thermoelectric element.

Robustness of PEDOT:Tos films

Wearable thermoelectric materials are expected to undergo mechanical stress during their use so they should be durable. We tested the durability of the nanorough PEDOT:Tos/PDAC/PET thermoelectric films by performing bending, creasing,

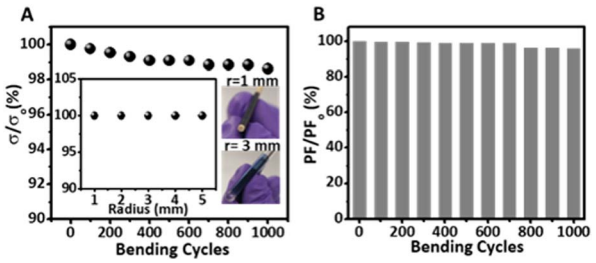

Fig. 4 (A) Relative electrical conductivity *vs.* bending cycles of a nanorough PEDOT:Tos/PDAC/PET film with a specific bending radius of 1 mm. Inset: the relative electrical conductivity of the nanorough PEDOT:Tos/PDAC/PET as a function of bending radius for one bending cycle and photos showing bending of the nanorough PEDOT:Tos/PDAC/PET films across a cylindrical rod with radius of 1 mm and 3 mm, and (B) relative power factor of the film before and after bending as a function of bending cycle with a bending radius of 1 mm.

adhesion, and washing tests (see ESI for details†). The test results indicated that the films could stay almost intact even after creasing, 1000 bending cycles, 20 adhesion tests, and 20 washing cycles using soap water. More specifically, we found that the resistance of the films was practically unaltered after creasing (Fig. S6†). Fig. 4 shows that the electrical conductivity and the relative power factor of the films were barely reduced after 1000 bending cycles around a 1 mm rod. Fig. S7† shows that the relative electrical conductivity and the power factor of the films stay almost unchanged after multiple adhesion tests. Fig. S8† shows that washing cycles do not damage the films as the relative electrical conductivity and power factors of the films remain almost the same.

Performance of complete thermoelectric device

To further explore how much power a PEDOT-based thermoelectric device can produce, we developed a proof-of-concept complete, flexible thermoelectric device (Fig. 2A and B) that is composed of strips of p-type organic thermoelectric material (*i.e.*, nanorough PEDOT:Tos/PDAC/PET) and strips of n-type thermoelectric material (*i.e.*, bismuth films deposited on PET films). Fig. 2D–F show the voltage and actual power produced by the device when the opposite sides of the device were subjected to different temperatures. We concluded that this simple proof-of-concept device can produce up to 118.7 nW when it is subjected to a temperature difference of 50 K, yielding a power density of 68.6 μW m^{-2}. We also measured the performance of the device under realistic conditions by just holding the device outdoor on a moderately mild warm day as well as a cold day. The device produced a voltage of 5.44 mV (a power output about 8.5 nW) by using the temperature difference between the bare hand of a user and an ambient temperature of 15 °C (Fig. 2G). When the outside temperature was −4.9 °C the voltage generated by the device was 8.13 mV (see Fig. S10 and Video in ESI†). The voltage of the device reached 8.73 mV when the device was held with a gloved hand. The thermoelectric power output produced by the device in all cases was stable for several minutes; we tested the device for 15 minutes on a moderately mild day (15 °C) and 5 and 20 minutes on a cold day (−5 °C) depending on whether the user was holding the device with a gloved hand or a bare hand.

Conclusions

The present study demonstrates that the thermoelectric performance of thin-film organic thermoelectrics is affected by the surface roughness of the thin films. Tailoring surface roughness could, therefore, be a simple and efficient approach to boost the efficiency of organic thermoelectrics. In this study, we also report a new soft templating method to fabricate rough films of organic thermoelectrics. The soft-templating method at first prepares a thin film of the organic thermoelectric film that has polystyrene nanobeads embedded. At a subsequent step the polystyrene nanobeads are dissolved and leave behind nanovoids that make the surface of the films rough. Even though we used the soft template method to fabricate only nanorough PEDOT:Tos films, we believe that this technique can be also used for the preparation of other nanorough organic thin films.

The nanorough PEDOT:Tos films that we prepared exhibited a *ZT* equal to 0.99 that is one of the highest ever reported. Notably, the soft templating method is simple and the nanorough thin films could be in principle easily mass produced. It should be also noted that the organic thermoelectric elements reported in the literature with higher *ZT* than that of nanorough PEDOT:Tos films were produced using multistep or technically difficult approaches[4,47] which might be difficult to scale up. The proof-of-concept thermoelectric device that used the nanorough PEDOT:Tos films was tested under realistic outdoor conditions, yielding promising results. Further research is, however, needed on the development of efficient n-type organic thermoelectric elements to be paired with the nanorough PEDOT:Tos films to allow the development of all organic, efficient thermoelectric devices suitable for wearable applications.

Data availability

The data supporting this article have been included in the figures of the manuscript or as part of the ESI.†

Conflicts of interest

There are no conflicts to declare.

Acknowledgements

This work was funded by U.S. Army Combat Capabilities Development Command Soldier Center (Contracts # W911QY-17-2-0004 and # W911QY-18-2-0006); this manuscript was approved for public release, PR2023-193. The authors would like to thank Earl Ada (Material Characterization Lab, University of Massachusetts Lowell) for help on AFM and SEM experiments.

References

1 S. J. Kim, J. H. We and B. J. Cho, *Energy Environ. Sci.*, 2014, **7**, 1959.
2 M. Hyland, H. Hunter, J. Liu, E. Veety and D. Vashaee, *Appl. Energy*, 2016, **182**, 518.
3 Z. Lu, H. Zhang, C. Mao and C. M. Li, *Appl. Energy*, 2016, **164**, 57.
4 C. Cho, B. Stevens, J. H. Hsu, R. Bureau, D. A. Hagen, O. Regev, C. Yu and J. C. Grunlan, *Adv. Mater.*, 2015, **27**, 2996.
5 J. Wang, K. Cai and S. Shen, *Org. Electron.*, 2015, **17**, 151.
6 Z. Fan and J. Ouyang, *Adv. Electron. Mater.*, 2019, **5**, 1800769.
7 I. Petsagkourakis, N. Kim, K. Tybrandt, I. Zozoulenko and X. Crispin, *Adv. Electron. Mater.*, 2019, **5**, 1800918.
8 H. Wang and C. Yu, *Joule*, 2019, **3**, 53.
9 B. Russ, A. Glaudell, J. J. Urban, M. L. Chabinyc and R. A. Segalman, *Nat. Rev. Mater.*, 2016, **1**, 16050J.
10 J. Tang, Y. Chen, S. R. McCuskey, L. Chen, G. C. Bazan and Z. Liang, *Adv. Electron. Mater.*, 2019, **5**, 1800943.
11 Z. Liao, X. Zhou, G. Wei, S. Wang, C. Gao and L. Wang, *ACS Appl. Mater. Interfaces*, 2022, **14**, 43421.
12 X. Li, R. Zou, Z. Liu, J. Mata, B. Storer, Y. Chen, W. Qi, Z. Zhou and P. Zhang, *npj Flexible Electron.*, 2022, **6**, 6.
13 C. Ou, A. L. Sangle, A. Datta, Q. Jing, T. Busolo, T. Chalklen, V. Narayan and S. Kar-Narayan, *ACS Appl. Mater. Interfaces*, 2018, **10**, 19580.
14 A. M. Routsi, T. Maji, C. Drew, J. Kumar and D. C. Christodouleas, *Appl. Mater. Today*, 2021, **25**, 101180.
15 T. Park, C. Park, B. Kim, H. Shin and E. Kim, *Energy Environ. Sci.*, 2013, **6**, 788.
16 O. Bubnova, Z. U. Khan, A. Malti, S. Braun, M. Fahlman, M. Berggren and X. Crispin, *Nat. Mater.*, 2011, **10**, 429.
17 J. Wang, K. Cai, H. Song and S. Shen, *Synth. Met.*, 2016, **220**, 585.
18 Z. U. Khan, O. Bubnova, M. J. Jafari, R. Brooke, X. Liu, R. Gabrielsson, T. Ederth, D. R. Evans, J. W. Andreasen, M. Fahlman and X. Crispin, *J. Mater. Chem. C*, 2015, **3**, 10616.
19 M. V. Fabretto, D. R. Evans, M. Mueller, K. Zuber, P. Hojati-Talemi, R. D. Short, G. G. Wallace and P. J. Murphy, *Chem. Mater.*, 2012, **24**, 3998.
20 I. Petsagkourakis, E. Pavlopoulou, G. Portale, B. A. Kuropatwa, S. Dilhaire, G. Fleury and G. Hadziioannou, *Sci. Rep.*, 2016, **6**, 30501.
21 S. R. S. Kumar, N. Kurra and H. N. Alshareef, *J. Mater. Chem. C*, 2016, **4**, 215.
22 N. Toshima, *Synth. Met.*, 2017, **225**, 3.
23 Q. Zhang, Y. Sun, W. Xu and D. Zhu, *Adv. Mater.*, 2014, **26**, 6829.
24 O. Bubnova, M. Berggren and X. Crispin, *J. Am. Chem. Soc.*, 2012, **134**, 16456.
25 B. T. McGrail, A. Sehirlioglu and E. Pentzer, *Angew. Chem., Int. Ed.*, 2015, **54**, 1710.
26 I.-L. Ngo, S. Jeon and C. Byon, *Int. J. Heat Mass Transfer*, 2016, **98**, 219.
27 Y. Xu, Y. Jia, P. Liu, Q. Jiang and D. Hu, *Chem. Eng. J.*, 2021, **404**, 126552.
28 F. Zhang, J. Song, M. Chen, J. Liu, Y. Hao, Y. Wang, J. Qu and P. Zeng, *Phys. Chem. Chem. Phys.*, 2016, **18**, 32903.
29 Y.-C. Wang, Y. Sun, D. Mei and Z. Chen, *Appl. Energy*, 2018, **215**, 690.
30 J. Liu, G.-M. Choi and D. G. Cahill, *J. Appl. Phys.*, 2014, **116**, 233107.
31 P. Martin, Z. Aksamija, E. Pop and U. Ravaioli, *Phys. Rev. Lett.*, 2009, **102**, 125503.
32 I. Hochbaum, R. Chen, R. D. Delgado, W. Liang, E. C. Garnett, M. Najarian, A. Majumdar and P. Yang, *Nature*, 2008, **451**, 163.
33 L. N. Maurer, Z. Aksamija, E. B. Ramayya, A. H. Davoody and I. Knezevic, *Appl. Phys. Lett.*, 2015, **106**, 133108.
34 S. N. Patel and M. L. Chabinyc, *J. Appl. Polym. Sci.*, 2017, **134**, 44403.
35 J. Liu, X. Wang, D. Li, N. E. Coates, R. A. Segalman and D. G. Cahill, *Macromolecules*, 2015, **48**, 585.
36 A. Weathers, Z. U. Khan, R. Brooke, D. Evans, M. T. Pettes, J. W. Andreasen, X. Crispin and L. Shi, *Adv. Mater.*, 2015, **27**, 2101.
37 Z. Tian, S. Lee and G. Chen, *Annu. Rev. Heat Transfer*, 2014, **17**, 425.
38 D. Hohnholz, A. G. MacDiarmid, D. M. Sarno and J. W. E. Jones, *Chem. Commun.*, 2001, **23**, 2444.
39 X. Guan, H. Cheng and J. Ouyang, *J. Mater. Chem. A*, 2018, **6**, 19347.
40 T. Witting, T. C. Chasapis, F. Ricci, M. Peters, N. A. Heinz, G. Hautier and G. J. Snyder, *Adv. Electron. Mater.*, 2019, **5**, 1800904.
41 G. J. Snyder and E. S. Toberer, *Nat. Mater.*, 2008, **7**, 105.
42 E. H. Khan, S. Thota, Y. Wang, L. Li, E. Wilusz, R. Osgood and J. Kumar, *J. Electron. Mater.*, 2018, **47**, 3963.
43 Y. Lu, Y. Qiu, K. Cai, Y. Ding, M. Wang, C. Jiang, Q. Yao, C. Huang, L. Chen and J. He, *Energy Environ. Sci.*, 2020, **13**, 1240.
44 E. Jin Bae, Y. Hun Kang, K.-S. Jang and S. Yun Cho, *Sci. Rep.*, 2016, **6**, 18805.
45 S. J. Kim, H. E. Lee, H. Choi, Y. Kim, J. H. We, J. S. Shin, K. J. Lee and B. J. Cho, *ACS Nano*, 2016, **10**, 10851.
46 L. Yang, Z.-G. Chen, M. S. Dargusch and J. Zou, *Adv. Energy Mater.*, 2018, **8**, 1701797.
47 C. Cho, K. L. Wallace, P. Tzeng, J.-H. Hsu, C. Yu and J. C. Grunlan, *Adv. Energy Mater.*, 2016, **6**, 1502168.